










ARTICLE

Warm Fog Artificial Dispersion, Preliminary Results

Alexandra Alekseeva¹ , Vladimir Davidov¹ , Vladimir Ivanov² , Aleksei Palei^{1*} , Yuri Pisanko^{1,3} ,
Anatoly Savchenko² , Marina Vasilyeva⁴ , Aleksei Vasilyev⁵ , Marina Zinkina¹ 

¹Geoeffective Radiation Department, Fedorov Institute of Applied Geophysics, Rostokinskaya st.9, Moscow 129128, Russia

²Department of Atmospheric Modelling, RPA Typhoon, Pobeda st.4, Obninsk 249038, Kaluga region, Russia

³Ocean's Thermo-Hydromechanics Chair, Moscow Institute of Physics and Technology (National Research University), Institutsky Lane 9, Dolgoprudny 141701, Moscow region, Russia

⁴Guarding and Management Chair, Russian University of Transport (MIIT), Obraztsova st.9, Moscow 127994, GSP-4, Russia

⁵Automatic Control System Chair, Bauman Moscow State Technical University (Bauman MSTU), Moscow 105005, Russia

ABSTRACT

We describe the results of laboratory and field experiments aimed at dispersing warm fog. The laboratory experiments were conducted inside the Large Aerosol Chamber (volume: 3500 m³) RPA Typhoon (Obninsk, Russia) while the field experiments were carried out in the Caucasus foothills (Nalchik, Russia) and foothills close to Usui-Karuizawa (Japan). The results of experiments in the Large Aerosol Chamber demonstrated that the ion wind generated by the corona discharge lifted the fog cloud from a height of 3 m to 12 m. In the installation area, the fog dissipated and the visibility range increased dramatically. Field experiments in the North Caucasus revealed that the method for fog displacement from a controlled area with air stream electrically cleared from fog droplets could only be recommended to disperse fog in the area located downwind of the object. At the same time, the fog flow velocity should also be no more than 5 m/s per second. Statistics of field experiments at foothills close to Usui-Karuizawa (Japan) indicated that the effect of corona discharge on warm fog manifested itself in a noticeable change in fog density and range of visibility. The methods of fog displacement with air mechanically purified from water droplets are also considered from the point of view of its potential technical solutions.

Keywords: Fog Artificial Dispersion; Electric Charge; Corona Discharge; Ion-Dipole Interaction; Condensation

*CORRESPONDING AUTHOR:

Aleksei Palei, Geoeffective Radiation Department, Fedorov Institute of Applied Geophysics, Moscow 129128, Russia; Email: a_paley@mail.ru

ARTICLE INFO

Received: 24 September 2024 | Revised: 28 March 2025 | Accepted: 9 April 2025 | Published Online: 22 April 2025

DOI: <https://doi.org/10.30564/jasr.v8i2.7247>

CITATION

Alekseeva, A., Davidov, V., Ivanov, V., et al., 2025. Warm Fog Artificial Dispersion, Preliminary Results. Journal of Atmospheric Science Research. 8(2): 51–64. DOI: <https://doi.org/10.30564/jasr.v8i2.7247>

COPYRIGHT

Copyright © 2025 by the author(s). Published by Bilingual Publishing Group. This is an open access article under the Creative Commons Attribution-NonCommercial 4.0 International (CC BY-NC 4.0) License (<https://creativecommons.org/licenses/by-nc/4.0/>).

1. Introduction

The issue of artificial effects on fogs attracts considerable attention in the literature; a detailed analysis can be found in Kachurin ^[1]. A fog not only limits visibility, but also worsens the quality of the road surface. The grip of the car with the road decreases, the handling of the car deteriorates, and, as a result, during the occurrence of fog, the probability of safe movement decreases. According to the US Federal Highway Administration (FHWA), limiting visibility on roads leads to a decrease in highway capacity by 10–12% ^[2]. Fog and smoke are indeed risk factors for this horrific and lethal crash type ^[3]. There are two fog classes: cold fogs and warm ones. We will concentrate on warm fogs. A few methods have been proposed for warm fog modification ^[4]. They include:

- hydroscopic seeding,
- treating warm water surfaces in the vicinity with chemicals to suppress evaporation and reduce the possibility of fog formation,
- mixing the fog layer with overlying warm dry air drought down by helicopter downwash,
- promotion of fog droplet coalescence by strong sound waves,
- evaporation of the fog droplets by heating with laser beams,
- introduction of charged particles to collect the fog droplets,
- the spreading of chemicals, e.g., surfactants, to modify the condensation processes (a kind of nuclei poisoning),
- the collection of large volumes of the fog filled air by suction devices, the removal of the fog droplets by screening and centrifuging and the exhaustion of the air, now free of fog droplets, back to the atmosphere.

We consider the methods of electrical action on fogs ^[5–11] and methods of displacing fog with air purified from water droplets ^[12–15] as promising ones to disperse warm fogs. One can ensure the electric effect on the fog by exposing it to an inhomogeneous electric field created near high voltage electrode ^[15], or by generating electric charges in the atmosphere using special devices ^[16–20].

2. Electrical Methods of Fog Dispersal

There are three types of electrical methods:

- fog dispersion with ion wind,
- fog displacement from a controlled area with air stream, which is electrically cleared from fog droplets,
- fog dispersion by direct exposure it with a corona discharge.

A corona discharge is an electrical discharge caused by the ionization of air surrounding a conductor carrying a high voltage. It represents a local region where the air has undergone electrical breakdown and become conductive, allowing charge to continuously leak off the conductor into the air. Ion wind is the airflow of charged particles induced by electrostatic forces linked to corona discharge arising at the tips of some sharp conductors subjected to high voltage relative to ground.

2.1. Fog Dispersion with Ion Wind

The physics, in principle, is simple: ions accelerated by the local electric field in the gas discharge collide with neutral molecules/atoms and cause them to move; this discrete collisions cascade to create a bulk medium motion. The effect is enhanced in water vapor due to large water dipole moment and ion-dipole electric interaction. To verify the ion wind concept and investigate its effectiveness, experimental work was carried out in a Large Aerosol Chamber (LAC) of RPA Typhoon (Obninsk). We measure the effectiveness of fog dissipation techniques by the time interval between the moment of turning on the installation and the moment of fog dissipation. The shorter is this time interval the more effective is the technique. The dimensions of the camera (diameter 15 m, height 18 m, volume 3,200 m³,) and the availability of appropriate technical systems make it possible to accurately simulate natural fogs and the processes of their dispersion natural and artificial. The chamber design and thermodynamic characteristics are described in detail in the research ^[21]. The measuring equipment is described in the research ^[22]. As a device for electro-physical exposure to fog, a laboratory installation with an area of 1.5 × 1.5 m² with a maximum electrical power of about 300 watts was used. The results of the research are described in detail in the research ^[23]. The photo

of the placement of an ion wind generating unit in LAC is shown in **Figure 1**.



Figure 1. The photo of the placement of the ion wind generating unit in the large aerosol chamber. 1—installation, 2—medium transparency meter based on a helium–neon laser ^[23].

When the installation was turned on, the fog dissipated during 20 seconds. The dynamics of the evolution of fog in the process of exposure is shown in **Figure 2**. The obtained experimental results allow us to conclude that the ion wind generated by the corona discharge lifts the fog cloud up (from the height of 3 m to the height of 12 m). In the installation area, the fog dissipates and the visibility range increases dramatically.

2.2. Fog Displacement from a Controlled Area With Air Stream Electrically Cleared from Fog Droplets

The schematic diagram of the device implementing air stream electrically cleared from fog droplets is presented in the research ^[24]. **Figure 3** shows its structural and layout scheme.

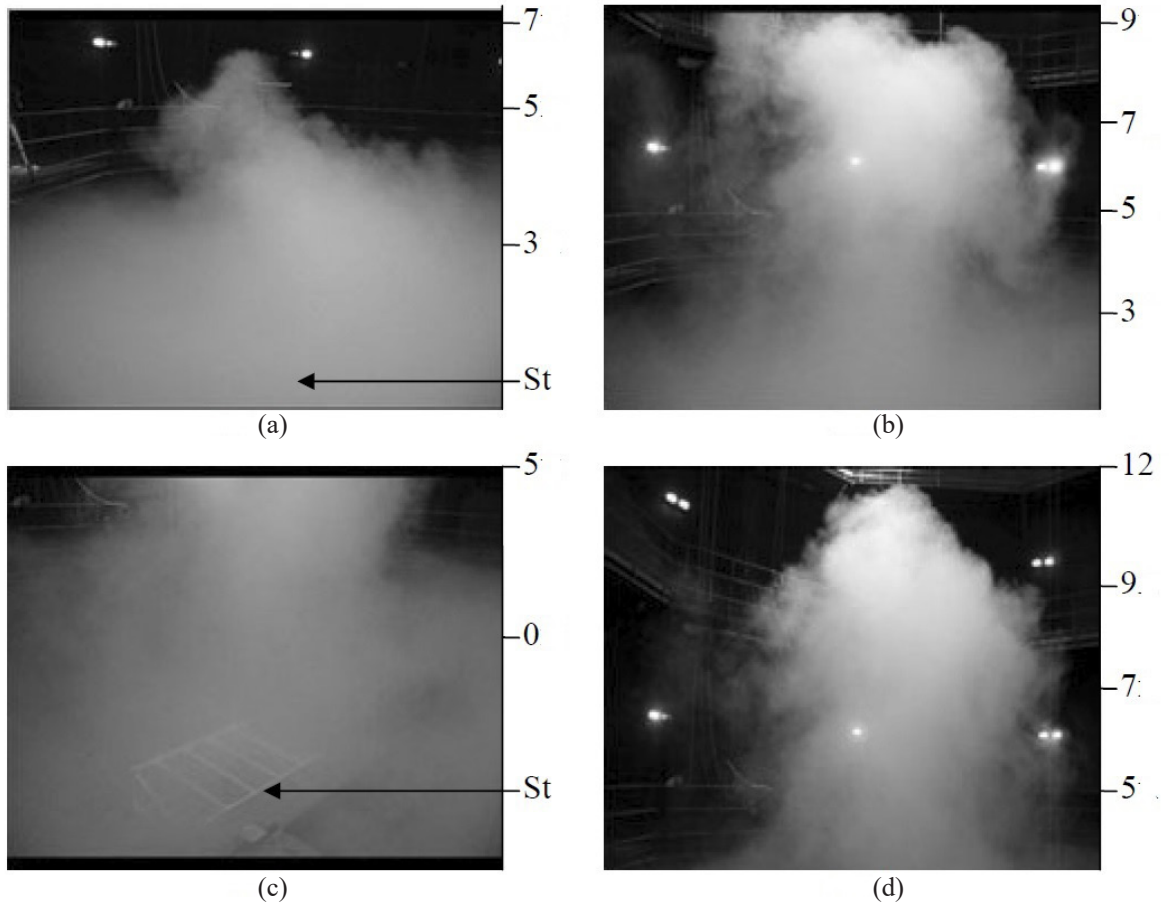


Figure 2. A visual picture of the evolution of fog during the operation of the installation, St is the installation location, the height (in meters) from the floor level of the camera is indicated on the right. (a) the fog dispersion unit is turned on; (b) 20-second of the installation (upstream view); (c) the 20th second of the installation (view of the installation); (d) the 30th second of the installation operation (view of the upstream) ^[23].

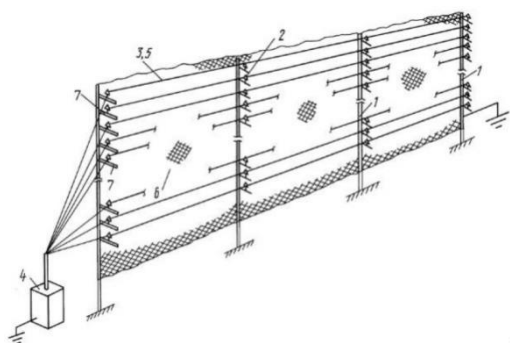


Figure 3. Structural and layout scheme of a device, which electrically clears air stream from fog droplets. 1—supports; 2—insulators; 3, 5—wires having a small radius; 4—high voltage source; 6—a grounded grid.

The principle of operation and the theoretical analysis of such a device are presented in the research [7]. The results of laboratory studies of the fog dispersal device were reported in 2013 [25]. Also, there were experiments [26] to investigate current-voltage and hydrodynamic characteristics in the air space close to the laboratory gauze electrostatic precipitator specimen, when generating the corona from alternating voltage with a frequency of 50 Hz in the range from 20 to 32 kV.

The precipitator consists of two horizontal electrodes: the grounded conductive gauze and the system of parallel corona wires. The latter is fixed with a gap of 7 cm relative to the grounded gauze. The fog, whose top reached the level of ~4.5 m from the floor, was generated by ultrasonic water dispersants after the formation of the stable temperature stratification in LAC (the difference in air temperature is about 2°C along the chamber height). The fog formation was created by decreasing air temperature while reducing preliminarily created overpressure. We carried out the experiments when the precipitator was situated below the fog. In natural conditions, we observed almost no changes in the density and boundaries of the generated fog for a long time (more than 20 minutes). After turning on the precipitator, the fog dissipated in several minutes. We controlled the fog dispersion with medium-phase two-way transmissometer based on the helium-neon laser with a wave length of 0.63 mm with a total base of 4 m. It was situated in the LAC at the height of 2 m from the floor and at the distance of 6 m from the precipitator. In other experiments, the precipitator with the downward electric field direction was installed above the fog in the center of the LAC at the heights varied from 3.5 to 6 m.

At the height of 2 m (below the precipitator), there was the platform (1.1 × 2 m) with temperature, humidity, and optical thickness sensors to measure droplet and aerosol sizes. We maintained the voltage between the electrodes in both experiments roughly equal to 30 kV so that electric currents varied within 3.6–4.0 μA, and the ion wind speed was within 1.1–1.2 m/s.

At the first stage, the studies followed the scheme where the grounded electrode made of metal gauze with the squared cell size of 10 × 10 mm was situated above, and the corona electrode was located below. When we apply the voltage of more than 24 kV, an upward flow (the ion wind from the corona discharge) takes place. The velocity of the upward air flow reaches ~1 m/s. At the second stage, we use the scheme where the corona electrode was situated above, and the grounded electrode (made of metal gauze with the squared cell size of 20 × 20 mm) was located below. In this case, the ion wind during the corona discharge was directed down (downward flow). We obtain that the current-voltage characteristics for the case of the downward air flow even slightly exceed the ones for the upward flow. One can explain the phenomenon by the fact that the aerodynamic resistance to the downward flow of the ion wind was smaller (the metal gauze cell size was 20 × 20 mm in the first case and 10 × 10 mm in the second case). We carried the additional experiment to study the nature of the phenomenon and to estimate the possible contribution of the thermal convection to the upward flow created by the ohm's heating of the corona electrode. Installed was the heating element of the working area of 1.5 × 1.5 m² and power consumption ~300 W. We measured the temperature and velocity of the thermal convection at the level of the output grounded electrode with the digital thermometer. The measurements did not indicate the velocity of thermal convection no more than 0.1 m/s, which corresponds to the level of the anemometer background signal. Hence, the contribution of the thermal convection can be neglected, and the main role in the fog dispersal belongs to the ion wind from the corona discharge.

In the research [7] presented are the theoretical dependencies describing the fog gathering by electric charging of fog's droplets. In particular, one can get from the research [7] how variations of both mesh structural element dimensions and air flow speed influence on the process

of water droplets collecting under various supplying high voltages. If there is no corona discharge, no water collection takes place. However, mesh is covered by water during a few seconds after the corona discharge is formed. In experiments lasting up to 10 hours, the technique of fog gathering by electric charging of fog's droplets demonstrate stable functioning.

During our experiment, the average radius of fog droplets increased from 2 to 6 μm at liquid water content from 0.2 to 1.3 g/m^3 . Note that the extent of fog clearing from droplets varied from 80 to 95%. The amount of 0.7 liters of water collected during 20 minutes is in accordance with clearing of 1300 m^3 fog water, which passed through a filter with the average liquid water content of 0.6 g/m^3 at electric energy consumption of $\approx 10^5$ J. At direct condensation of water from air, this amount of energy will be sufficient for obtaining only of ≈ 40 mL of water. The effect of the laboratory installation on the change in the optical transparency of the fog is shown in **Figure 4**.

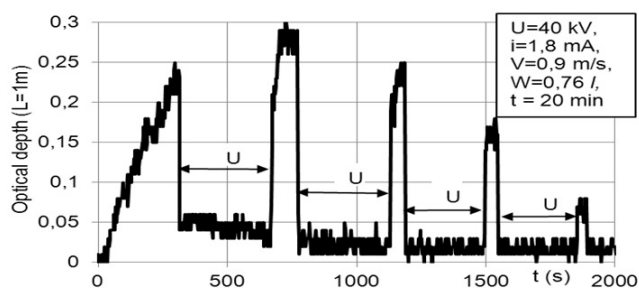


Figure 4. Changes in fog optical depth along the base of 1 m at switching of a corona discharge (marked by two-sided arrows) ^[25].

An experimental sample of such a device was mounted and tested at Nalchik airport (**Figure 5**, Nalchik city, North Caucasus, Russia, 2015).



Figure 5. Experimental fog dispersion facility (Nalchik city, 2015).

Figure 6 shows the process of fog dispersion using this experimental installation.

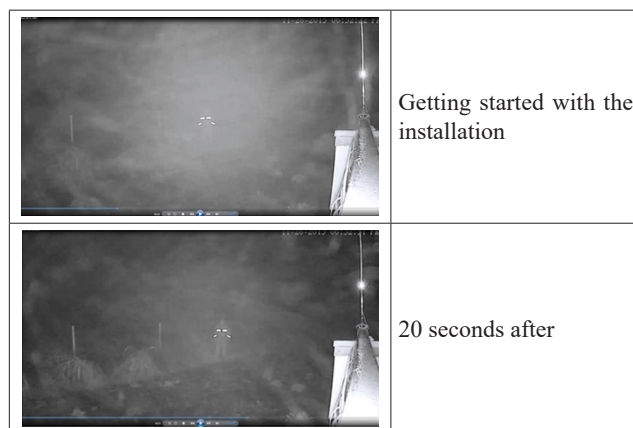


Figure 6. Fog dispersion due to the operation of installation. A man is located at a distance of 25 meters from the installation.

The west winds impede the meridional circulation preserving cold north atmospheric fronts at North Caucasus for a long time. North atmospheric fronts lead to cold air flows along the mountains facilitating cloudiness there. During winter time (October–March), cold wet Caspian air moves to North Caucasus. Both factors form fogs and low stratified cloudiness in the place of experiment. There are 135 fogs during a year at the place, mostly warm fogs in November and March, lasting from 3 hours to 4.5 hours in average. Laboratory and field tests have demonstrated the high efficiency of the method for fog displacement from a controlled area with air stream electrically cleared from fog droplets. However, the method can only be recommended to disperse fog in the area located downwind the object. At the same time, the fog flow velocity should also be limited to a value of no more than 5 m per second. Proposals ^[27] for the further development of the method are aimed to increase the efficiency of corona discharge generation.

2.3. Fog Dispersion by Direct Exposure to a Corona Discharge

The technology of fog direct exposure by electric charges is based on the mechanism of ion-dipole interaction of water molecules with electrically charged particles ^[11,28,29]. The fog dispersal experimental installation was mounted in the framework of an agreement on joint research with a Japanese heavy engineering company “Ishikawajima Harima” (IHI) in Usui-Karuizawa in 1993–1996 in Japan.

The place for the installation was chosen in the mountains on one of the parking lots of the expressway, at an altitude of about 800 meters above the sea level. Fog occurs at the installation site from April to October, which, due to the presence of established rules for driving on expressways in Japan, leads to a decrease in speed or even a complete stop of movement. The total lifetime of fogs with the visibility range of less than 1000 meters for 4 years of observations was 4020.17 hours (taking into account the operation of the fog dispersion unit in 1996). The idea is that the application of high voltage on the wires causes the corona discharge, which provides electrical charging of atmospheric aerosol particles. Charged aerosol particles move partly towards the ground, according to the direction of the electric field lines. On their way the charged particles capture the molecules of water and molecular complexes, which, colliding with water drops make the latter large enough for their gravitational precipitation. All these processes provide the fog dispersion.

The experimental installation included the corona discharge generation source and the control panel with the high voltage source. The corona discharge generation system consisted of corona wires mounted on insulators of high-voltage supports. Three corona wires were attached to each row of supports. The central wire is installed at a height of 6.0 meters. Two side wires are installed symmetrically relative to the central wire on the crossbar. The design of the crossbar and its attachment to the supports allows adjusting the position of the side wires both in height and in relation to the axis of the central wire. The supports were installed on a mountain slope near the expressway. A detailed description of the installation is provided in the patents for the invention: USA (US6152378); Canada (CA2268842) and in the European patent (EP1010810). In particular, we measured spatial scales of aerosol before and during installation functioning. Because the visibility decrease is initiated by fog's droplets of average spatial scale of 3–5 micrometer we measured aerosol variation in the range 0.5–1000 micrometers by LDSA-1400 spectrometer. The particles with a size of 0.15–0.2 microns, 0.2–0.3 microns, and 0.3–0.5 microns, we measured by JIAC-PC-95 aerosol spectrometer and ДАЭС-2М electrostatic counter of fine aerosol. The devices were installed outdoors at the distance of 1.5 meters from the installation as well as me-

teorology devices.

The results of experimental studies in laboratory and field conditions have shown that electric charges have a significant effect on the evolution of the dispersion of atmospheric aerosol particles (both in fog and in clear weather conditions). When corona discharges are generated into the atmosphere at an atmospheric humidity of 80%, an increase in the concentration of particles with a size of 0.2–0.3 microns and 0.3–0.5 microns is revealed (see **Figure 7**), while the concentration of particles with a size of 0.15–0.2 microns decreases. This can be explained by the fact that water particles condense on dry particles with a size of 0.15–0.2 microns after the generation of corona discharges; this leads to an increase in the size of initially dry particles. In support of this process, a decrease in atmospheric humidity was noted. Field experiments have shown that, when exposed to a corona discharge, fogs with a visibility range of less than 150 meters practically dissipated, and the lifetime of fogs with a visibility range of less than 300 meters is significantly (almost twice) reduced (see **Figure 8**).

We turned on the apparatus for 25 minutes continuously in case of the humidity higher than 90%, and for 5 minutes continuously in case of the visibility less than 1000 m. Otherwise, we turned off the apparatus. Sometimes, randomly, we turned off the apparatus during the periods of humidity higher than 90% and the periods of visibility less than 1000 m to obtain the natural background of fog dispersal. The results of artificial fog dispersal, we estimated statistically. We gathered the statistics of fog (with visibility below 1000 m) occurrence in the place of the experiment for 1993, 1994, 1995, and 1996. Totally, the fog took place during 4020.17 hours in this place. In every year, we separated the spring fog (April–July) from the fall one (August–October). We denoted as 100% the total time of fog existence during each of these eight temporal intervals. In each of eight temporal intervals, we separated the time periods during which the visibility was below 50, 70, 100, 150, 200, 300, and 500 m. We compared the time periods (expressed in percent) of fog of given visibility under the natural fog dispersion (the installation was turned out) with the time periods of the same visibility when the installation was turned on. We used the measurements of visibility from four observational points: the first – in the

place of installation, the second – two km downwind from the installation, the third – 3 km downwind from the installation, the fourth – 5 km downwind from the installation. There were many fogs at the four observational points in 1993–1996. The fog of visibility less than 500 m took place during 47.17 hours at the first observational point, 52.5 hours at the second observational point, 76.33 hours at the third observational point, and 47.17 hours at the fourth observational point.

The fogs of less than 100 m visibility occupied minimum 3.91% (August–October 1995) while increased up to more than 10% (April–July 1993 and April–July 1996) of total time of fog existence. During the installation functioning, the percentage of such fogs decreased to 0.35%. The fogs of less than 150 m visibility occupied minimum 8% while sometimes increased up to 20%. During the installation functioning, the percentage of such fogs decreased to 1.22%. The fogs of less than 200 m visibility occupied up to 10% (August–October 1994). During the installation functioning, the percentage of such fogs decreased to 3.49%. The fogs of less than 300 m visibility occupied up to 15.61% (August–October 1994). During the installation functioning, the percentage of such fogs decreased to 7.59%.

We compared the fog natural dissipation during four years and the fog artificial dissipation due to the installation functioning (**Figure 8**). One can see from **Figure 8** that the installation functioning did not influence on the fog of visibility less than 500 m at the fourth observational point situated at the distance of 5 km downwind from the first observational point with the installation. However, the installation contributed to the dispersion of fogs of visibility less than 300 m at the second and third observational points.

The effect of corona discharge on warm fog manifests itself in a noticeable change in the characteristics of the fog (density, range of visibility). When the installation works, the probability of dense fog occurrence significantly decreases. So we concluded that there was the change in the microphysical parameters of the atmosphere during the generation of corona discharge, which had a noticeable effect on the time of fog dispersion. Therefore, by generating corona discharges in the atmosphere, meteorological conditions in an area with an increased probability of fog formation can be significantly improved. In more detail, the results of a full-scale experiment on fog dispersion on the road in Japan are presented in the research ^[29–30].

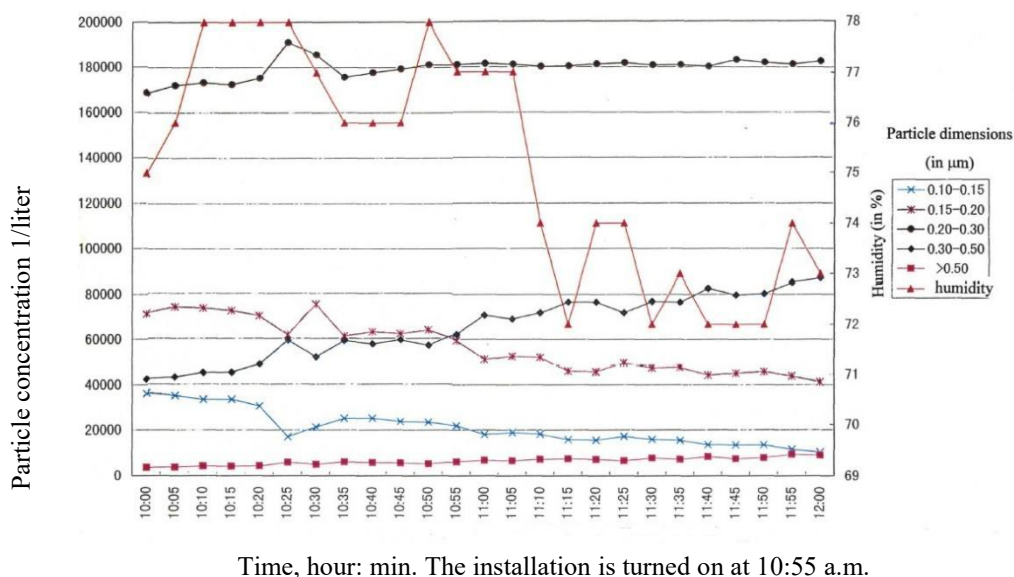
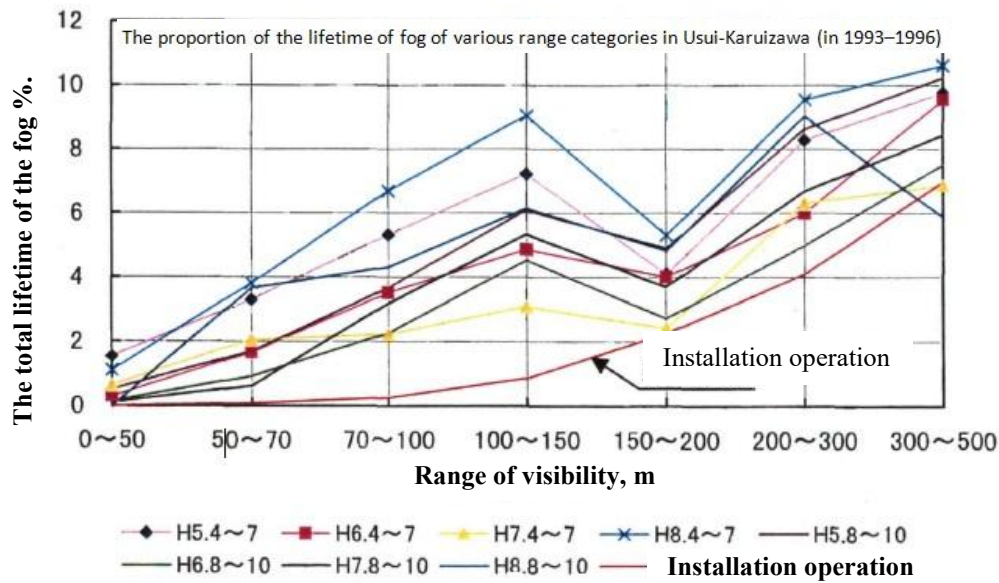


Figure 7. Changes in the concentration of aerosol particles during the experiment ^[29].



H5.4—April–July 1993; H6.4—April–July 1994; H7.4—April–July 1995; H8.4—April–July 1996; H5.8—August–October 1993; H6.8—August–October 1994; H7.8—August–October 1995; H8.8—August–October 1996.

Figure 8. The proportion of the lifetime of fog of various range categories in Usui-Karuizawa (in 1993–1996) ^[29].

3. Methods of Fog Displacement with Air Purified from Water Droplets

We consider the dispersion of fog by displacing it from a controlled area with air purified from water droplets as one of the promising ways to solve the problem of fog dispersion on a road. The principle of artificial fog dispersion on the road differs slightly from the request for conventional air ventilation and can be solved by practically known conventional technical means used in ventilation systems. It is only necessary to form large volumes of air with no fog droplets in the space surrounding a road, which is completely covered with fog. Unfortunately, attempts to use a conventional helicopter placed above the upper boundary of the fog are not always successful. A clean stream of air, moving through the fog, becomes clogged with fog droplets when approaching the road surface. The fog does not dissipate. Our proposals are aimed at finding technical solutions that ensure the separation of water droplets contained in the fog.

There are known technical solutions where fog is passed through a grid. Droplets of water, touching the structural elements of the grid, gather on their surface, enlarge and flow down, and the air flow cleared of water droplets moves in the direction of the wind. Structurally,

such devices can be made in the form of a flat grid, as shown in **Figure 9**.



Figure 9. Collection of water droplets, made in the form of a flat mesh ^[31].

In these devices, only those droplets that touch the surfaces of the structural elements of the grid during the flow movement are separated from the flow. At the same time, the air flows around the structural elements when passing through the grid. Since the droplets are small, the aerodynamic forces, which are proportional to the square of the droplet size, significantly exceed the inertial forces, which are proportional to the cube of the droplet size.

$$k = \frac{F_v}{F_i} = \frac{k_1 r^2}{k_2 r^3} = \frac{k_1}{k_2 r} \quad (1)$$

where F_v is the aerodynamic force; F_i is inertial force; r is the characteristic size of the drop; k , k_1 , k_2 are constant coefficients.

For a small drop (droplet) whose size is $r \rightarrow 0$, the value of $k \rightarrow \infty$. That is, droplets are frozen into the stream and flow around the obstacle practically along the lines of the current of air stream. To analyze the efficiency of collision of drops with the surface of structural elements of the mesh and, accordingly, the efficiency of water collection, one can use the Stokes criterion ^[32]:

$$S_{tk} = \frac{\lambda}{2R} = \frac{\rho \varpi_0 d^2}{18\mu 2R} \quad (2)$$

where λ —inertial path of a drop in the air; R —mesh structural element radius; ρ —density of water; ϖ_0 —speed of air flow incident on the mesh; d —drop diameter; μ —dynamic air viscosity.

According to the theory of inertial deposition ^[32], at low values of the Stokes number S_{tk} (for particles of small size and low mass), the particles precisely follow the lines of air flow without coming into contact with the frontal part of the streamlined body. Due to turbulent vortices, only a small part of finely dispersed drops can fall on the rear part of the streamlined surface. Thus, to increase the probability of collision of fog droplets with the surface of the structural elements of the mesh, and, consequently, to increase the efficiency of droplet separation, it is necessary to increase the Stokes number. Under conditions of given velocities of air masses and the range of sizes of fog droplets, the adjustable parameters are:

- radius of the mesh structural element: the thinner the fibers, the higher the Stokes number, and the higher the droplet collection efficiency. The design and layout diagram of a device that implements this method of increasing the efficiency of collecting drops is presented in the Russian Federation patent for the invention Ru 2746587 C1 (see **Figure 10**);
- the speed of the air flow incident on the structural element of the mesh (ϖ_0): this speed can be increased by moving the mesh relative to the air flow. Design and layout diagrams of devices that implement this method of increasing the efficiency of drop collection are presented in the RF patent

for the invention Ru 2781216 C1 (see **Figure 11**).

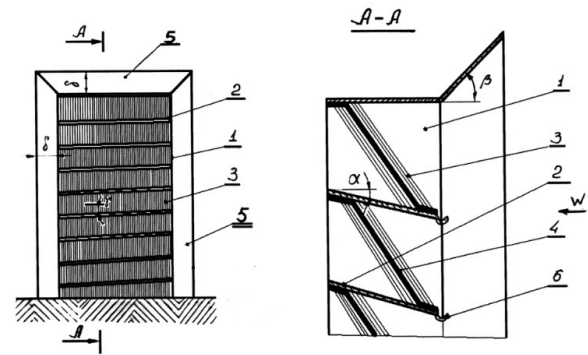


Figure 10. Device for droplet separation. 1—racks; 2—waterproof partition; 3—filter element; 4—frame; 5—dynamic reflectors; 6—groove for draining the separated liquid.

The device includes a frame made in the form of racks 1 facing each other. Partitions 2 are installed between the racks 1 above each other at an angle α to the horizon and with a gap δ between them. A filter element 3 is fixed in the gap between the partitions 2. The filter element 3 is made of a bundle of randomly stacked thin steel wires assembled in the form of a plate or tape laid and fixed on a frame 4 made in the form of a grid with cells. The size of the mesh cell is selected at the design stage from the condition of reliable attachment of the filter material on it, reliable attachment of the forming filter element 3 in the gap between the partitions 2 and minimal aerodynamic drag for the passage of air flow. In the experiments conducted by the inventors, the size of the grid cell was at least 2 mm. The thickness of the grid frame elements, its structural design and its dimensions are selected at the design stage depending on the gap between the partitions 2, the thickness of the plate layer, the tape, the degree of its density and the number of layers to be laid. **Figure 10** shows a variant of the grid frame, made in the form of a plate, on the surface of which a layer of tape is laid from a bundle of randomly stacked thin steel wires. The grid frame can also be made in the form of a cylindrical surface, a cone, a parallelepiped, etc. surfaces that are technologically convenient for fixing tape layers on them and mounting the formed structure in the gap between the partitions 2. Most of the steel wires are oriented in them in the shared direction of the tapes. The laying of the metal tape is carried out in such a way that most of the fibers of thin steel wires are oriented on the fog dispersion device in a plane vertical to

the surface of the Earth. In the figure, the fibers are conventionally depicted in the idea of thin lines, indicated by position 3. A metal tape or plate can be made similarly to a well-known special metal material that is used for finishing polishing products. This is the so-called steel wool (in the literature its name is also found as “iron wool”, “metal wool”, “steel wool”, “steel wool”, “iron wool”, “wire wool”, “steel wire”, “wire sponge”, etc.), which is a bundle of randomly stacked steel wires with a diameter of no more than 1 mm.

As the number of droplets deposited on the surface of the fibers increases, they become larger and, under the influence of gravitational forces, flow down to the partition 2 and then along the groove 6 are removed from the device. Considering that most of the fibers of thin steel wires are oriented vertically on the fog dispersion device, the resistance to the downward movement of droplets under the influence of gravity is reduced. The number of pores filled with water decreases, which facilitates freer passage of air flow through the filter element (its aerodynamic resistance is reduced).

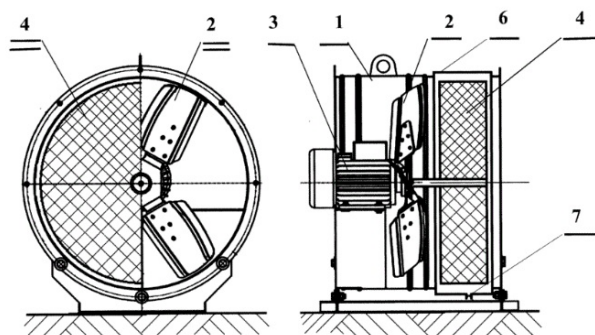


Figure 11. Drip separation device with a fan. 1—air duct; 2—fan blades; 3—drive axis; 4—a filter element made in the form of a porous, open-pore structure; 5—a shell; 6—a drainage hole.

The fog dispersal device contains a fan with a drive installed in the air duct 1, which includes fan blades 2 mounted on the drive axis 3. A filter element made in the form of a porous, open-pore structure is also attached to the drive axis 3. A porous (open-pore) structure can be made according to known design schemes of spatial structures, made with gaps between structural elements that allow air flow to pass through it, for example, in the form of wheel spokes (see <https://www.google.com/>

[search?q=spokes+wheels](https://www.google.com/search?q=spokes+wheels)), or in the form of a spatial structure woven (with a gap between each other) from thin wire, by analogy with known schemes (see <https://daly.ru/katalog/kapleulovitel-ultraset/>). It can also be made of porous, open-pore material, for example, foamed polyurethane (<https://ffvm.ru/produktsiya/penopoliuretan-dlya-filtrov-ppu.php>). The main requirement for the filter element is the presence of open pores for air flow to pass through it and the separated liquid to move through its pores from the axis to the periphery, as well as the absence of imbalance when it rotates on the drive axis. The size of the open pores of the filter material is determined at the design stage depending on the rotation speed of the fan drive, the required degree of purification of the gas flow and restrictions on the aerodynamic resistance of the air flow in air duct 1. To eliminate the imbalance of the porous structure with open pores, it is most convenient to make it in the form of a disk 4, as shown in **Figure 11**, attached to the blades of fan 2. A shell 5 is attached to the body of the air duct 1, in the area surrounding the porous structure with open pores (a disk made of porous material with open pores 4). The shell 5 is made with a length no less than the thickness of the disk 4, and its internal diameter exceeds by at least 5 mm the internal diameter of the housing 1. A drainage hole 6 is made in the lower part of the shell 5.

Considering that the porous structure with open pores in the devices, presented in **Figure 11**, rotates at the speed of rotation of the fan blades 2, drops of water contained in the air flow being purified are captured by the structural elements of the pores impinging on them and deposited on their surface. The relative speed of movement between the fog droplets and the pore structural elements, which determines the probability of the fog droplets colliding with the structural elements, is determined by the rotational speed of the fan drive. By increasing the rotation speed of the fan motor, you can achieve almost any predetermined degree of fog purification from droplets.

Fog dispersal devices that implement the principle of replacing fog with air purified from fog droplets can be made in the form of stationary modules mounted along the road surface or in the form of mobile devices, the diagrams of which are presented in **Figures 12 and 13**.

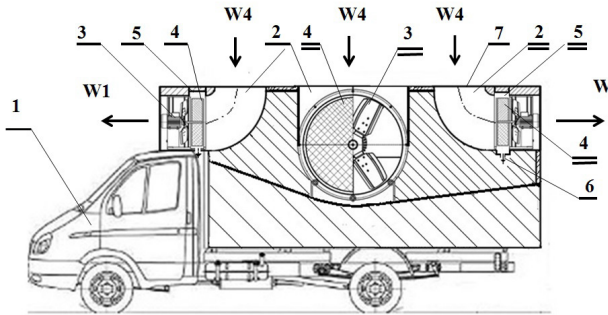


Figure 12. Mobile fog dispersal device. 1—car; 2—air channel; 3—fan installed with a drive; 4—filter element; 5—shell; 6—drainage hole; 7—air intake.

The system for forming air flows cleared of fog droplets includes a fan installed in the air channel 2 with a drive 3, on the axis of which a filter element 4 is fixed, made in the form of a porous rotating disk with open pores. In the air channel 2, in the area surrounding the porous rotating disk 4 with open pores, a shell 5 is inserted. The shell 5 is made in length no less than the thickness of the disk 4, and its internal diameter exceeds the internal diameter of the air duct 2 by at least 5 mm. In the lower part of the shell 5 there is a drainage hole 6. For air intake, an air intake 7 is made in the upper part of the device, connected to the air channel 2. To prevent any foreign objects from entering the air channel 2, the air intake 7 can be covered with an air-permeable mesh. This technical tool allows you to solve the problem of dispersing warm fog on the road, without installing special equipment on it, which reduces the costs of both equipment installation and operation. Similarly, technical means that ensure the formation of a jet of air purified from fog droplets can be installed on an unmanned aerial vehicle. This provides a perspective to solve the problem of fog dispersion in any given area.

The fog disperser consists of a housing 1 and power units for generating directional airflow 2. Each power unit for generating directional airflow 2 includes a fan impeller 5 mounted on the axis 3 of the engine 4, mounted in the air channel 6. A mist droplet separation device is installed in the air channel 6 over an area overlapping its cross-section. The device for separating mist droplets is presented in the form of a porous disk with open pores 7, rigidly mounted on the axis 3 of the engine 4. The implementation of a mist droplet separation device in the form of a porous disk with open pores mounted on the axis of the engine makes it possible to reduce its aerodynamic resistance to the air flow

generated by the impeller of the fan in the air channel. A drainage hole 8 is mounted in the lower part of the air duct 6 to drain fog droplets.

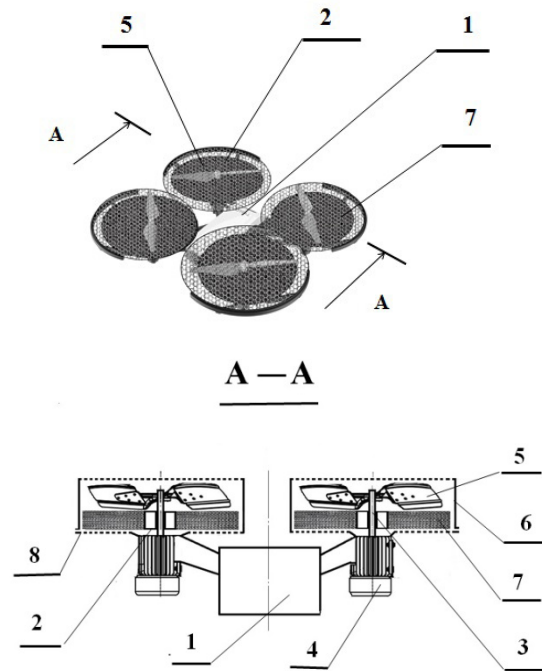


Figure 13. Fog dispersal mobile device, based on an unmanned aerial vehicle. 1—housing; 2—power units for generating directional airflow; 3—axis of the engine; 4—engine; 5—fan impeller; 6—air channel; 7—porous disk with open pores; 8—drainage hole.

The proposed aircraft for fog dispersion works as follows. When fog occurs, the aircraft takes off into an area controlled by fog. The flight of the aircraft is carried out using power units mounted on the body 1 for generating directional airflow 2, the operation of which is provided by a power source and regulated by a control system. The air containing mist droplets is taken from the space above the aircraft by the impeller of the fan 5 of the power units for generating directional airflow 2 and through the air channel 6 is directed to a porous open-pore filter element installed in the air channel 6, which in **Figure 13** is presented in the form of a rotating porous open-pore disk 7. Fog drops collide with the structural elements of the pores of the rotating filter element, adhere to them and separate from the air flow. The air stream, cleared of fog droplets, is carried down, forming a reactive force that ensures the movement of the aircraft, and displaces the fog from the area over which the aircraft is currently flying with the pressure of

its jet. Fog droplets, deposited on the structural elements of the pores, as they pass through the porous surface of disk 7, become larger. Under the action of centrifugal forces, fog droplets are thrown against the walls of the air channel 6. Under the action of gravity, the droplets flow down to the drainage hole 8 and are discharged outside. The air flow coming out, cleared of fog droplets, displaces the fog from the area over which the aircraft is currently flying by the pressure of its jet. As the aircraft moves forward with a system mounted on it for the formation of air flows cleared of fog droplets, the area is cleared of fog. Thus, the proposed technical solution makes it possible to solve the problem of effective dispersion of warm mists in a controlled area and ensures the achievement of this goal.

4. Conclusions

1. It is shown that artificial methods of warm fog dispersal are realizable.

2. The results of experiments in the Large Aerosol Chamber allow us to conclude that the ion wind generated by the corona discharge lifts the fog cloud up (from the height of 3 m to the height of 12 m). In the installation area, the fog dissipates and the visibility range increases dramatically.

3. Field experiments at North Caucasus revealed that the method for fog displacement from a controlled area with air stream electrically cleared from fog droplets could only be recommended to disperse fog in the area located downwind the object. At the same time, the fog flow velocity should also be limited to a value of no more than 5 m per second.

4. Statistics of field experiments at foothills close to Usui-Karuizawa (Japan) revealed that the effect of corona discharge on warm fog manifested itself in a noticeable change in the characteristics of the fog (density, range of visibility). When the installation worked, the probability of dense fog occurrence significantly decreased.

5. There are several promising methods of fog displacement with air mechanically purified from water droplets. These can be realized by technical means mounted both on cars and on pilotless vehicles.

Author Contributions

Conceptualization, A.P.; methodology, A.P.; valida-

tion, A.A. and M.Z.; formal analysis, V.D., A.V., and M.V.; investigation, A.A., V.D., V.I., Y.P., A.S., and M.Z.; writing—original draft preparation, A.P., and Y.P.; writing—review and editing, A.P., and Y.P. All authors have read and agreed to the published version of the manuscript.” Authorship must be limited to those who have contributed substantially to the work reported.

Funding

This work received no external funding.

Institutional Review Board Statement

Not applicable.

Informed Consent Statement

Not applicable.

Data Availability Statement

Data are available from the authors under request.

Conflicts of Interest

The authors declare no conflict of interest.

References

- [1] Kachurin, L.G., 1990. Physical grounds of influence on atmospheric processes. Gidrometeoizdat: Leningrad, Russia. p. 464. (in Russian).
- [2] U.S. Department of transportation Federal Highway Administration, 2024. How Do Weather Events Affect Roads? Available from: https://ops.fhwa.dot.gov/weather/q1_roadimpact.htm (cited 30 April 2025)
- [3] Hamilton, B., Tefft, B., Arnold, L., et al., 2014. Fog and Traffic Crashes on America's Roads. Available from: <https://aaafoundation.org/wp-content/uploads/2017/12/FogAndCrashesReport.pdf> (cited 30 April 2025).
- [4] Dennis, A.S., 1980. Weather Modification by Cloud Seeding. In: Hales, A.L. (eds.). International Geophysical. Academic Press Inc.: New York, NY, USA. pp. 1–267.
- [5] Li, D., Li, C., Xiao, M., et al., 2025. Sustainable solutions for water scarcity: a review of electrostatic fog harvesting technology. Communications Engineering, 4, 34. DOI: <https://doi.org/10.1038/s44172->

025-00381-x

- [6] Frost, W., 1982. Preliminary Test Results of Electrical Charge Particle Generator for Application to Fog Dispersal. Available from: <https://ntrs.nasa.gov/citations/19830006552> (cited 30 April 2025).
- [7] Damak, M., Varanasi, K.K., 2018. Electrostatically driven fog collection using space charge injection. *Science Advances*. 4(6), eaao5323. DOI: <https://doi.org/10.1126/sciadv.aao5323>
- [8] Frost, W., Collins, F., Koepf, D., 1981. Charged Particle Concepts for Fog Dispersion. Available from: <https://ntrs.nasa.gov/citations/19810018106> (cited 30 April 2025).
- [9] Li, D., Li, C., Li, J., et al., 2022. Efficient corona discharge fog collector multiple mesh electrodes with electric field enhances fog harvesting. *Plasma Chemistry and Plasma Processing*. 42, 1249–1264. DOI: <https://doi.org/10.1007/s11090-022-10279-7>
- [10] Lapshin, V.B., Yablokov, M.Yu., Palei, A.A., 2022. Vapor pressure over a charged drop. *Russian Journal of Physical Chemistry*. 76(10), 1727–1729.
- [11] Choi, J.S., Song, J.S., Choi, J.C., et al., 2012. Fog removal system. Available from: <https://patents.justia.com/patent/20130299603> (cited 30 April 2025).
- [12] Vasilyeva, M.A., Ivanov, V.N., Palei, A.A., et al., 2021. A method of fog dispersal. The RF patent for the invention RU2759763C1. Available from: <https://patents.google.com/patent/RU2759763C1/ru?oq=RU2759763C1> (cited 30 April 2025).
- [13] Vasilyeva, M.A., Ivanov, V.N., Palei, A.A., et al., 2022. A method for a gas stream cleaning from mist droplets. The RF patent for the invention Ru 2767611 C1 Available from: <https://patents.google.com/patent/RU2767611C1/ru?oq=RU+2767611+C1> (cited 30 April 2025).
- [14] Alekseeva, A.V., Vasiliev, A.S., Zinkina, M.D., et al., 2022. Device for fog dispersing. The RF patent for the invention Ru 2781216 C1. Available from: <https://patents.google.com/patent/RU2781216C1/ru?oq=RU+2781216+C1> (cited 30 April 2025).
- [15] Alekseeva, A.V., Vasiliev, A.S., Danelian, B.G., et al., 2024. Element of the high-voltage electrode for the fog dispersion device on the road. The RF Utility model patent Ru225701U1. Available from: <https://patents.google.com/patent/RU225701U1/ru?oq=patent+Ru225701U1> (cited 30 April 2025).
- [16] Ju, J.J., Wang, T.J., Li, R.X., et al., 2017. Corona discharge induced snow formation in a cloud chamber. *Scientific reports*. 7, 11749. DOI: <https://doi.org/10.1038/s41598-017-12002-5>
- [17] Alekseeva, A.V., Vasiliev, A.S., Zinkina, M.D., et al., 2023. Device for electric charges into the atmosphere generating. The RF patent for the invention Ru 2794966 C1. Available from: <https://patents.google.com/patent/RU2794966C1/ru?oq=RU+2794966+C1> (cited 30 April 2025).
- [18] Alekseeva, A.V., Vasiliev, A.S., Zinkina, M.D., et al., 2023. Device for unipolar electric charges into the atmosphere generating. The RF patent for the invention Ru 2807518 C1. Available from: <https://patents.google.com/patent/RU2807518C1/ru?oq=RU+2807518+C1> (cited 30 April 2025).
- [19] Alekseeva, A.V., Vasiliev, A.S., Zinkina, M.D., et al., 2023. Device for electric charges into the atmosphere generating. The RF patent for the invention Ru 2807519 C1. Available from: <https://patents.google.com/patent/RU2807519C1/ru?oq=RU+2807519+C1> (cited 30 April 2025).
- [20] Alekseeva, A.V., Vasiliev, A.S., Zinkina, M.D., et al., 2024. A device for fog dispersing by droplets separating. The RF patent for the invention Ru 2814625 C1. Available from: <https://patents.google.com/patent/RU2814625C1/ru?oq=RU+2814625+C1> (cited 30 April 2025).
- [21] Romanov, N.P., Zhukov, G.P., 2000. Thermodynamic relations for a fog chamber. *Russian Meteorology and Hydrology* 10, 37–52.
- [22] Romanov, N., Erankov, V., 2013. Calculated and experimental regularities of cloud microstructure formation and evolution. *Atmospheric and Climate Sciences*. 3(3), 301–312. DOI: <https://doi.org/10.4236/acs.2013.33032>
- [23] Lapshin, V.B., Vasilyeva, M.A., Zhokhova, N.V., et al., 2009. Test results of the electro-physical method of fog dispersion in a large aerosol chamber Scientific and Production Association Typhoon. *Researched in Russia Magazine*. 20, 718–726. (in Russian).
- [24] Lapshin, V.B., Ogarkov, A.A., Palei, A.A., et al., 1999. A device for fogs and clouds dispersing. The RF patent for the invention Ru 2124288 C1 Available from: <https://patents.google.com/patent/RU2124288C1/ru?oq=RU+2124288+C1> (cited 30 April 2025).
- [25] Palei, A.A., Romanov, N.P., 2013. A Construction and Characteristics of a Fog Droplet Collector made with the Use of a Corona Discharge. In *Proceedings of the Sixth International Conference on Fog, Fog Collection and Dew*; 19–24 May, 2013; Yokohama. Japan. p.19.
- [26] Andreev, Yu.V., Vasilyeva, M.A., Ivanov, V.N., et al., 2021. Results of Experimental Studies on the Dispersal of Warm Fogs Using Gauze Electrostatic Precipitators. *Russian Meteorology and Hydrology*. 46(10), 716–721.
- [27] Reznikov, M., 2015. Electrically enhanced condensation I: Effects of corona discharge. *IEEE transactions on industry applications*. 51(2), 1137–1145. DOI: <https://doi.org/10.1109/tia.2014.2354734>
- [28] Harrison, R.G., Marlton, G.J., Maarten, H., et al., 2022. Modifying natural droplet systems by charge

- injection. *Physical review research*. 4, L022050. DOI: <https://doi.org/10.1103/PhysRevResearch.4.L022050>
- [29] Lapshin, V.B., Palei, A.A., Yablokov, M.Yu., 2004. Experimental studies in laboratory and field conditions of the effect of corona discharge on the evolution of aerosol dispersion and fog density. *Researched in Russia Magazine*. 200, 2129–2140. (in Russian).
- [30] Lapshin, V.B., Palei, A.A., 2006. Results of field experiments to estimate the influence of corona discharge on fog density. *Russian meteorology and hydrology*. 1, 29–33. DOI: <https://doi.org/10.31857/S0207401X2001015X>
- [31] Moncuquet, A., Mitranescu, A., Marchand, O.C., Ramanarivo, S., Duprat, C., 2022. Collecting fog with vertical fibres: Combined laboratory and in-situ study. *Atmospheric Research*, 277, 106312. <https://doi.org/10.1016/j.atmosres.2022.106312>
- [32] Vetoshkin, A.G., 2019. *Fundamentals of environmental engineering*. Penza university publishing, Penza, Russia. p. 452. (in Russian).